NATIONAL ADVISORY COMMITTEE FOR AERONAUTICS

TECHNICAL NOTE 2196

EFFECT OF HEAT-CAPACITY LAG ON THE FLOW THROUGH OBLIQUE SHOCK WAVES

By H. Reese Ivey and Charles W. Cline

Langley Aeronautical Laboratory
Langley Air Force Base, Va.

Washington
October 1950

NATIONAL ADVISORY COMMITTEE FOR AERONAUTICS

TECHNICAL NOTE 2196

EFFECT OF HEAT-CAPACITY LAG ON THE FLOW THROUGH OBLIQUE SHOCK WAVES

By H. Reese Ivey and Charles W. Cline

SUMMARY

An analysis is made of the effects of variable heat capacity on the flow parameters for oblique shock waves at high supersonic speeds at sea level. Two sets of results are obtained: one corresponding to conditions immediately behind the shock wave where only the active degrees of freedom of the molecules are in equilibrium; and another representing the asymptotic conditions far behind the shock wave where all the degrees of freedom are in equilibrium.

The flow characteristics behind strong oblique shock waves are shown to depend upon the distance downstream of the wave as well as the Mach number and flow deflection. The density distribution at high speeds is many times as sensitive to heat-capacity changes as the pressure distribution. The effect of heat-capacity variation is expected to be of increasing significance at higher altitudes.

The study of heat-capacity effects was used as background information to derive a very simple expression for predicting pressures due to shock waves and expansion waves at Mach numbers from 1.3 to ∞. The pressure equation is applied to several problems and is shown to be surprisingly accurate.

INTRODUCTION

As the speeds and altitudes of missiles increase, the ranges of applicability of many aerodynamic theories are exceeded and more rigorous theories must be used not only in calculating the forces on aircraft but also in designing and calibrating instrumentation and experimental equipment. Reference 1 began the derivation of a simple theory for calculating the pressures over various shapes at hypersonic speeds. In the theory of reference 1 the simplifying assumption was made that the ratio of specific heats of the gas was 1.0. For that particular ratio the various integrations involved were readily performed and a very simple expression was obtained for calculating the pressure over airfoils and bodies of revolution. The curves of pressure against flow deflection obtained have the proper trends; however, the effect of specific-heat ratio on the magnitude of the pressures needs further study.

Bethe and Teller (reference 2) have generalized the theory of shock waves to the case where the specific heat changes with temperature. The methods of quantum statistics were used to calculate the distribution of energy among the various degrees of freedom for different densities and temperatures. The equilibrium energy distribution was used to determine the equilibrium conditions far behind normal shock waves. Two sets of conditions were presented: one set of conditions immediately behind the shock wave, corresponding to a constant ratio of specific heats; and another set of conditions far behind the shock wave where the energy is distributed according to equilibrium considerations. Reference 2 adds appreciably to the understanding of strong shock waves; however, the results are not in the simplest form for application to efficient aircraft where most of the shock waves are oblique. Because the flow deflection is zero in all normal shock waves, reference 2 does not show the effect of the heat-capacity variation on the shock-wave angle for a given flow deflection.

The purpose of the present paper is to present the results of Bethe and Teller in a form more directly applicable to oblique shock waves. The effects of heat-capacity variation on the flow conditions around wedge airfoils are investigated. The results of the study are used to derive a simple expression for calculating the pressure coefficients due to shock waves and expansions at Mach numbers from 1.3 to ∞.

SYMBOLS

M	Mach number
P	pressure coefficient
v	velocity, feet per second
α	angle of attack, degrees
β	wedge angle, degrees
β'	flow deflection angle, degrees
γ	ratio of specific heats
δ	semiwedge angle, degrees
θ	shock-wave angle, degrees
ρ	density (without subscript, behind shock wave), slugs per cubic foot

Subscripts:

a	approximate
e	exact
n	normal to shock wave
1	in region 1
2	in region 2
3	in region 3
∞	in free stream

ANALYSIS AND DISCUSSION

Effect of Heat-Capacity Lag

The properties of an oblique shock wave can be related to the properties of a normal shock wave by the equation

$$\frac{\rho}{\rho_\infty} = \frac{\tan \theta}{\tan(\theta - \beta')} \tag{1a}$$

where

ρ	density behind wave
ρ_∞	density in front of wave
θ	shock-wave angle
β'	flow deflection

In classical shock-wave theory, the specific heats are assumed to remain constant throughout all regions of flow. For such flow conditions, the density ratio ρ/ρ_∞ is determined from the Mach number normal to the shock wave by the equation

$$\frac{\rho}{\rho_\infty} = \frac{\gamma + 1}{\gamma - 1 + \frac{2}{M_n^2}} \tag{1b}$$

The Mach number normal to the wave is defined as

$$M_n = M_\infty \sin \theta \qquad (2)$$

At very high flight speeds the air is heated during the shock compression to such high temperatures that the specific heats can no longer be considered (even approximately) constant throughout the entire region. The specific heats change from their low-temperature value in front of the shock wave to an equilibrium value far behind the shock wave in the following manner: The air enters the shock wave at the initial conditions of temperature, density, and pressure. Five degrees of freedom, three translational and two rotational, are active. In an extremely short distance (of the order of a mean free path) the air is compressed and heated to a very high temperature. A great deal of energy has been transmitted to the random energy of the molecules but, because of the short distance in which the compression has taken place, an insufficient number of collisions have occurred to excite any inert degrees of freedom. The air flow, consequently, follows the pattern predicted by simple shock-wave theory in this region immediately behind the shock.

The air at this point is at a very high temperature. Collisions between molecules are occurring frequently and at very high speeds; consequently, the vibrational degree of freedom begins to absorb energy from the strong collisions. As time passes, the vibrational degree of freedom begins to store up appreciable energy. In time the vibrations become sufficiently strong to cause dissociation of the molecules into atoms. Now, if the temperature, which decreases as each new degree of freedom absorbs energy from the random motion of the molecules, is still sufficiently high, further collision of the dissociated atoms with other atoms or with molecules will cause ionization, which may be considered another degree of freedom. In general, the air comes to some equilibrium condition with energy distributed in definite proportions to the various degrees of freedom and with the temperature sufficiently high to cause the frequency and strength of the particle collision to be adequate to maintain this energy distribution.

Bethe and Teller (reference 2) have generalized the theory of normal shock waves to the case where the specific heat changes with temperature. The properties of a normal shock wave cannot be converted to those of an oblique shock wave for the condition of variable specific heats as easily as they can in classical shock-wave theory because the effect of variable conditions behind the wave must be considered. The properties of the air flow with variable specific heat, however, can be determined for three regions about a wedge airfoil by a fairly simple analysis of the conditions which govern the flow pattern at these three points. These regions are illustrated in figure 1 and are discussed in detail in the following paragraphs:

Region 1: The first case to be considered deals with the flow behind the leading shock wave and in the immediate vicinity (within a few mean free-path lengths) of the nose of the wedge (region 1). In passing through the shock wave in this region the molecules have their energy distributed among the active degrees of freedom. Immediately after passing through the wave and before the energy has had sufficient time to be distributed by molecular collisions to any degrees of freedom other than the original five, the flow is forced to follow the surface of the wedge. Consequently, the fluid, forced to deflect to the wedge angle before γ has had sufficient time to change from 1.4, behaves in a manner that can be calculated by classical shock-wave theory. Figure 2, taken from reference 3, is a plot of the shock-wave angles for $\gamma = 1.4$ and is applicable in this region.

Region 2: The second case to be considered deals with the flow at a point on the wedge far behind the nose (region 2). The distance of this point from the wedge nose is sufficiently large to cause the shock-wave thickness plus the relaxation distance to appear only as a thickened shock wave far ahead of the point. Furthermore, the influence of the part of the shock wave near the nose of the wedge is negligible in comparison with the effects of all the other parts of the shock wave in the forward Mach cone from the point. Thus, the angle of the shock wave far from the nose of the wedge must be such as to yield a flow parallel to the surface in region 2, where the density is that which results from the heat capacities having reached equilibrium conditions as predicted in reference 2. Figure 3, computed with the use of reference 2, and equations (1a) and (2), is applicable for computing the shock-wave angle θ. To the left of the dashed line in figure 3 the curves are the same as those of figure 2; however, the parts of the curves on the right of the dashed line are in the range of varying specific heats and are different from those of figure 2, the difference increasing with deflection angle and Mach number. Figures 2 and 3 indicate the large error which would result from use of classical shock-wave theory to compute Mach number from shock-wave-angle measurements at very high free-stream Mach numbers. For instance, for a flow deflection of 20°, which sets up a shock-wave angle of 25° (far from the nose), classical theory predicts a Mach number of 15 (fig. 2); whereas the theory allowing for variable specific heats predicts a Mach number of 11 (fig. 3). This difference in the calculated Mach numbers indicates that, although the effect of variation of γ on the flow properties may be small, it may be equal to or greater than the effect of variations in Mach number at these high speeds. This fact should be kept in mind during any testing at high Mach numbers or testing in gases other than air.

Region 3: The third case deals with the flow immediately behind the shock wave but far behind the nose of the wedge (region 3). In this region, the shock-wave angle has already been determined by the boundary conditions in region 2. The heat capacities have not yet had sufficient

time to change appreciably and, consequently, the flow properties can be predicted by classical shock-wave theory. The flow deflection will be smaller than is required to cause the stream to be parallel to the wedge surface. Figure 2 is applicable in this region; however, here the shock-wave angle θ is known (from region 2), and the flow deflection is unknown; whereas in region 1 the opposite was true.

As an example of the three cases consider a wedge with a 30° slope at a Mach number of 10 at sea level:

Case 1: At the nose of the wedge the shock-wave angle is 38.5° (fig. 2) if boundary-layer effects are ignored.

Case 2: Far from the nose of the airfoil the shock-wave angle is 37° (fig. 3).

Case 3: The flow deflection immediately behind the shock wave but far from the nose of the airfoil is about 28.8° for the 37° shock-wave angle (fig. 2).

The previous discussion has dealt only with certain limiting cases of the flow parameters and gives no insight into the distance required to approach equilibrium and no determination of the curvature of the shock wave. Bethe and Teller indicate that the translation and rotation come into thermal equilibrium after one or a few collisions. From 20 to 500,000 collisions are necessary to establish vibrational equilibrium, depending on the vibrating molecule (nitrogen or oxygen) and the humidity of the air. Water vapor acts somewhat like a catalyst in increasing the efficiency of the collisions in redistributing the energy. For normal shock waves at sea level, the distance required for the vibration to reach equilibrium lies between 3 and 0.0016 millimeters. For oblique shock waves, the relaxation distance is actually greater because the flow velocities are higher; however, when measured normal to the shock wave, the distance is the same for normal and oblique shocks. The dissociation requires from 1 millimeter to 1 meter to reach equilibrium for the normal shock at sea level. At altitudes above sea level, more dissociation occurs at a given temperature, and also fewer collisions in a given distance. The effects of heat-capacity variation and lag, therefore, may take on added significance at high altitudes.

In simple cases, the flow parameters follow an exponential law in approaching equilibrium. If the shock wave is strong enough to cause dissociation on the high-pressure side, the vibration gradually approaches equilibrium, and then, much more slowly, the dissociation approaches equilibrium. The curvature of the shock wave is related to the rate at which the various degrees of molecular freedom approach equilibrium. If equilibrium is established rapidly, the shock wave must change from its initial angle to the final angle in a short distance. Hence, the wave will be

curved appreciably over the short distance and then will be fairly straight beyond that point. If the shock wave is strong enough to require several different regions of flow, each of extent determined by the rate of approach of a particular degree of freedom to equilibrium, then the shock wave will have several distinct parts, each related to one of the regions of flow. The magnitude of the changes in shock-wave angle is small and the wave forms a continuous curve.

A study of figures 2 and 3 indicates that maximum deflections of as much as about 45° are possible with attached shock waves when the specific heat is constant; whereas deflections of over 50° are possible when the specific heat reaches equilibrium. Because the flow near the leading edge behaves as though the specific heat remains constant, the deflection at the leading edge must be less than the lower limit (the value for constant γ). The slope of the surface can increase behind the leading edge as the specific heat varies without causing the shock to detach.

Figures 4 and 5 give the density ratios across oblique shock waves with constant and variable specific heats, respectively. These figures result from equations (1a), (1b), and (2), and table VIII of reference 2. As an example of the use of these figures consider the previously studied problem of the flow over a 30° slope at a Mach number of 10:

Case 1: At the nose of the wedge the density ratio across the shock wave is 5.33 (fig. 4).

Case 2: Far behind the nose of the wedge the density ratio has increased to 6.08 (fig. 5).

Case 3: Far from the nose of the wedge but immediately behind the shock wave the density ratio is 5.27. (See fig. 4 and use the flow deflection of 28.8° previously determined for this case.)

Figure 4 shows how the flow density ratio immediately behind the shock wave approaches the classical limiting value of 6 as the shock waves become stronger. In contrast, figure 5 gives no indication that a limiting value exists far behind the shock wave. Calculations similar to those of reference 2 can be used to extend the curves to higher Mach numbers where the dissociation is more and where electronic excitation is significant. The curves should not be extrapolated without actual calculations because the trend of the curves may change every time a new degree of freedom is excited.

From considerations of continuity of mass flow, the ratio of the velocity components normal to oblique shock waves is equal to the reciprocal of the density ratios across the waves. The velocity components tangential to the waves are the same before and after the wave. Because

the shock-wave angle from figure 2 or 3 and the corresponding density ratio from figure 4 or 5 are known, the velocity ratio across the wave is easily obtained. These velocity ratios are plotted in figures 6 and 7. For the flow over a 30° slope at a Mach number of 10:

Case 1: At the nose of the wedge the velocity ratio across the shock wave is 0.791 (fig. 6).

Case 2: Far behind the nose of the wedge the velocity ratio has increased to 0.804 (fig. 7).

Case 3: Far from the nose of the wedge but immediately behind the shock wave the velocity ratio is 0.812 (fig. 6).

The variation in heat capacity increases the change in density across a given shock wave. For the flow over a wedge, the increase in density decreases the required shock-wave angle. The effects of increased density and decreased wave angle largely cancel insofar as the velocity of the flow is concerned.

Bethe and Teller have given the pressure ratios across normal shock waves with and without the variation in heat capacity. The pressure coefficient for the oblique shock waves can immediately be determined by use of the previously determined Mach numbers for oblique shock waves of a strength equal to the normal shock waves of Bethe and Teller. These coefficients are presented in figures 8 and 9. The flow over a 30° slope at a Mach number of 10 can be determined by use of these figures:

Case 1: At the nose of the wedge the pressure coefficient is 0.628 (fig. 8).

Case 2: Far behind the nose of the wedge the pressure coefficient has dropped to 0.610 (fig. 9).

Case 3: Far from the nose of the wedge but immediately behind the shock wave the pressure coefficient is 0.596. (See fig. 8 at a deflection of 28.8°.)

The pressure coefficient is very insensitive to the variation in heat capacity experienced in most oblique shock waves. In fact, for thin airfoils at sea level no effect of heat-capacity change is to be expected below a Mach number of 20. Even at a Mach number of 100 the effect is small. At higher altitudes where more dissociation might be expected for equilibrium conditions and where the relaxation distance may be long, the effect of heat-capacity lag or heat-capacity variation might be significant, particularly for blunt objects such as a pitot tube.

With the previous information in mind, the accuracy of the calculated shock-wave properties may be discussed. Bethe and Teller's paper

suggests that the authors have used all known corrections in calculating the heat capacity at high temperatures; however, apparently they did not consider their results sufficient for the determination of the speed of sound behind strong shock waves. Because Bethe and Teller work with the total heat content of the gas, the determination of the speed of sound would require differentiation of some of their numerical quantities and the results might therefore be appreciably less accurate than their other results. Thus, the Mach number behind strong oblique shock waves cannot be accurately calculated from the work of reference 2. Reference 4, although not as rigorous as the work of Bethe and Teller, possesses the advantage that the specific heats are explicitly given for any flow condition; hence, the Mach number behind the shock can be calculated from this reference.

The density ratio across the shock wave is fairly sensitive to the change in specific heat and, therefore, would be less accurate than many of the other shock-wave parameters. Bethe and Teller, however, consider density ratios sufficiently accurate to publish; therefore, the pressure coefficient which is very insensitive to a small error in heat capacity would be extremely accurate. The actual relaxation distance is greatly affected by small changes in the atmosphere such as change in humidity; thus, the distances estimated in the present paper give only the order of magnitude of the relaxation distance. For many cases, the relaxation distance is sufficiently small for its effects near the nose of the airfoil to be masked by the boundary-layer growth in this region.

Derivation of Pressure Equation

Existing theories such as the linearized theory or Busemann's power series (reference 5 with the third coefficient corrected) form a simple means for calculating pressure distributions at low or moderate supersonic speeds. Where a solution in explicit form is not required, the more tedious shock-expansion method or characteristic method may be desirable in order to obtain an accurate solution for the higher Mach numbers. For curved airfoils, rotation of the flow at high supersonic speeds must be considered. The rotational flow over wings and bodies at infinite Mach numbers for a ratio of specific heats equal to 1.0 has been discussed in reference 1. The present paper furnishes additional information on the effect of heat-capacity variation. Figure 10 indicates the range of application over which linearized theory and Busemann's power series are reasonably accurate. The linearized theory is reasonably accurate up to a free-stream Mach number of approximately 2, and the power series retains its accuracy up to $M_\infty = 10$ for two terms and $M_\infty = 15$ for three terms. Within these limits these equations are useful in the determination of airfoil properties because they can be readily differentiated and integrated with respect to β'. It is preferable to use the simple theories wherever possible. At

higher Mach numbers where the variation in specific heats becomes significant, it is desirable to have an equation which gives the pressure coefficient as an explicit function of the flow deflection, free-stream Mach number, and effective ratio of specific heats. The purpose of the present section is to derive an equation of this type. In order for such an equation to be of value it should possess as nearly as possible the simplicity of the linearized theory and the accuracy of the shock-wave solution and it should apply over a very large Mach number range.

The derivation begins by consideration of the following relation for the density ratio across an oblique shock wave:

$$\frac{\rho_1}{\rho_\infty} = \frac{\tan\theta}{\tan(\theta - \beta')} = \frac{\gamma + 1}{\gamma - 1 + \frac{2}{M_\infty^2 \sin^2\theta}} \tag{3}$$

where

θ shock-wave angle

β' flow deflection

M_∞ Mach number ahead of shock wave

γ ratio of specific heats

In the first part of the derivation the deflection is assumed to be small and, hence, the tangent of β' can be taken as β'. The shock-wave angle θ is assumed small enough to be approximated by a two-term series (that is, M_∞ is large). Expanding equation (3), dropping the smallest terms, such as θ^3, β'^2 and $\frac{\beta'}{M_\infty^2}$, and solving for θ gives

$$2\theta = \frac{\gamma + 1}{2}\beta' + \sqrt{\left(\frac{\gamma + 1}{2}\beta'\right)^2 + \frac{4}{M_\infty^2}} \tag{4}$$

This expression gives the shock-wave angle accurately at moderate and high supersonic speeds where the assumptions are permissible. From shock-wave theory, the expression for the pressure coefficient is

$$P = \frac{2 \sin\theta \sin\beta'}{\cos(\theta - \beta')} \tag{5}$$

Substituting the value of θ from equation (4) and keeping significant terms gives

$$P = 2\beta'\theta = \beta'\left(\frac{\gamma + 1}{2}\beta' + \sqrt{\left(\frac{\gamma + 1}{2}\beta'\right)^2 + \frac{4}{M_\infty^2}}\right) \tag{6}$$

The equation is now valid only for large Mach numbers and must be modified before being useful at lower speeds. At low supersonic speeds equation (6) simplifies to

$$P \cong \frac{2\beta'}{\sqrt{M_\infty^2}} \tag{7}$$

whereas from linearized theory

$$P = \frac{2\beta'}{\sqrt{M_\infty^2 - 1}} \tag{8}$$

Making this correction to the pressure equation yields

$$P = \beta'\left(\frac{\gamma + 1}{2}\beta' + \sqrt{\left(\frac{\gamma + 1}{2}\beta'\right)^2 + \frac{4}{M_\infty^2 - 1}}\right) \tag{9}$$

Figure 11 shows that this equation is a good approximation at Mach numbers above approximately 1.5 and at lower Mach numbers is more accurate than the linearized theory. Even at extremely high Mach numbers the equation yields accurate results. In order to obtain the greatest accuracy from this equation, the proper value of γ should be used. This value may be obtained for sea-level conditions by use of equations (1a) and (1b) and figure 3. In order to be perfectly rigorous, a new value of γ should be computed for each deflection angle and Mach number. This procedure, however, is more involved than the accuracy of the equation warrants, and in actual computations, a value of γ computed for an average deflection angle and a given Mach number give satisfactory accuracy over a large range of deflection angles. The restrictions to the use of equation (9) are that the shock wave must be attached and the deflection must be small.

Busemann's series expression for pressure coefficient (reference 5) shows that to the second order in the deflection the same expression should hold for expansion waves and shock waves. Hence, equation (9) should be valid for weak expansion waves. Figure 12 indicates that the

pressure equation checks the exact Prandtl-Meyer equation for expansions between $M = 1.5$ and 20. Above Mach number 20, the pressure coefficient due to an expansion is negligible by comparison with the shock-wave pressure for the same deflection. Below $M = 1.5$, the present theory is more accurate than the corresponding linearized expression. For expansions, β' is considered negative and, hence, the absolute magnitude of the pressure coefficient is less for expansions than for compressions. For the case of $M_\infty = \infty$, the present theory is exact for both shock waves and expansions. For that case, the pressure coefficient for a shock wave becomes

$$P = (\gamma + 1)\beta'^2$$

and for an expansion,

$$P = 0$$

Figure 13 compares a pressure distribution over a double wedge airfoil as calculated by the present method with the pressures computed by the shock-expansion method of reference 3 for $\gamma = 1.4$. The agreement is good.

Figures 14 and 15 give the lift and drag coefficients, respectively, for single-wedge airfoils with semiwedge angles of 1°, 2°, and 3° at various angles of attack as calculated by two methods: the shock-expansion method using variable γ; and the present pressure equation. The present theory gives good agreement in both trend and magnitude.

In cases where rotational flow need not be considered, the present method yields satisfactory results for shock waves, expansion waves, or complete airfoils. For curved airfoils at high supersonic speeds, some of the ideas of reference 1 may possibly be employed to modify the approximate method of the present paper in such a way that the rotation of the flow can be taken into consideration in a simple manner.

A part of the approximate pressure-coefficient equation predicts the shock-wave angle. Where the equation is used for expansions, the same terms specify the location of a fictitious negative shock wave located between the terminal Mach lines of the actual expansion.

CONCLUDING REMARKS

The work of Bethe and Teller on the properties of strong normal shock waves has been extended to oblique shock waves for facilitating studies of the effect of heat-capacity variation on efficient aerodynamic shapes at high supersonic speeds. The significant conclusion

is that the heat-capacity variation should not be noticeable on thin airfoils below a Mach number of 20 although it may modify the flow over a blunt body at a Mach number as low as 2 at sea level. At higher altitudes heat-capacity lag may be noticeable.

The study of heat-capacity effects was used as background information to derive a very simple expression for predicting pressures due to shock waves and expansion waves at Mach numbers from 1.3 to ∞. The pressure equation is applied to several problems and is shown to be surprisingly accurate.

Langley Aeronautical Laboratory
National Advisory Committee for Aeronautics
Langley Air Force Base, Va., June 7, 1950

REFERENCES

1. Ivey, H. Reese, Klunker, E. Bernard, and Bowen, Edward N.: A Method for Determining the Aerodynamic Characteristics of Two- and Three-Dimensional Shapes at Hypersonic Speeds. NACA TN 1613, 1948.

2. Bethe, H. A., and Teller, E.: Deviations from Thermal Equilibrium in Shock Waves. Rep. No. X-117, Ballistic Res. Lab., Aberdeen Proving Ground, 1945.

3. Ivey, H. Reese, Stickle, George W., and Schuettler, Alberta: Charts for Determining the Characteristics of Sharp-Nose Airfoils in Two-Dimensional Flow at Supersonic Speeds. NACA TN 1143, 1947.

4. Eggers, A. J., Jr.: One-Dimensional Flows of an Imperfect Diatomic Gas. NACA TN 1861, 1949.

5. Sauer, Robert: Introduction to Theoretical Gas Dynamics. J. W. Edwards, Ann Arbor, 1947, p. 197.

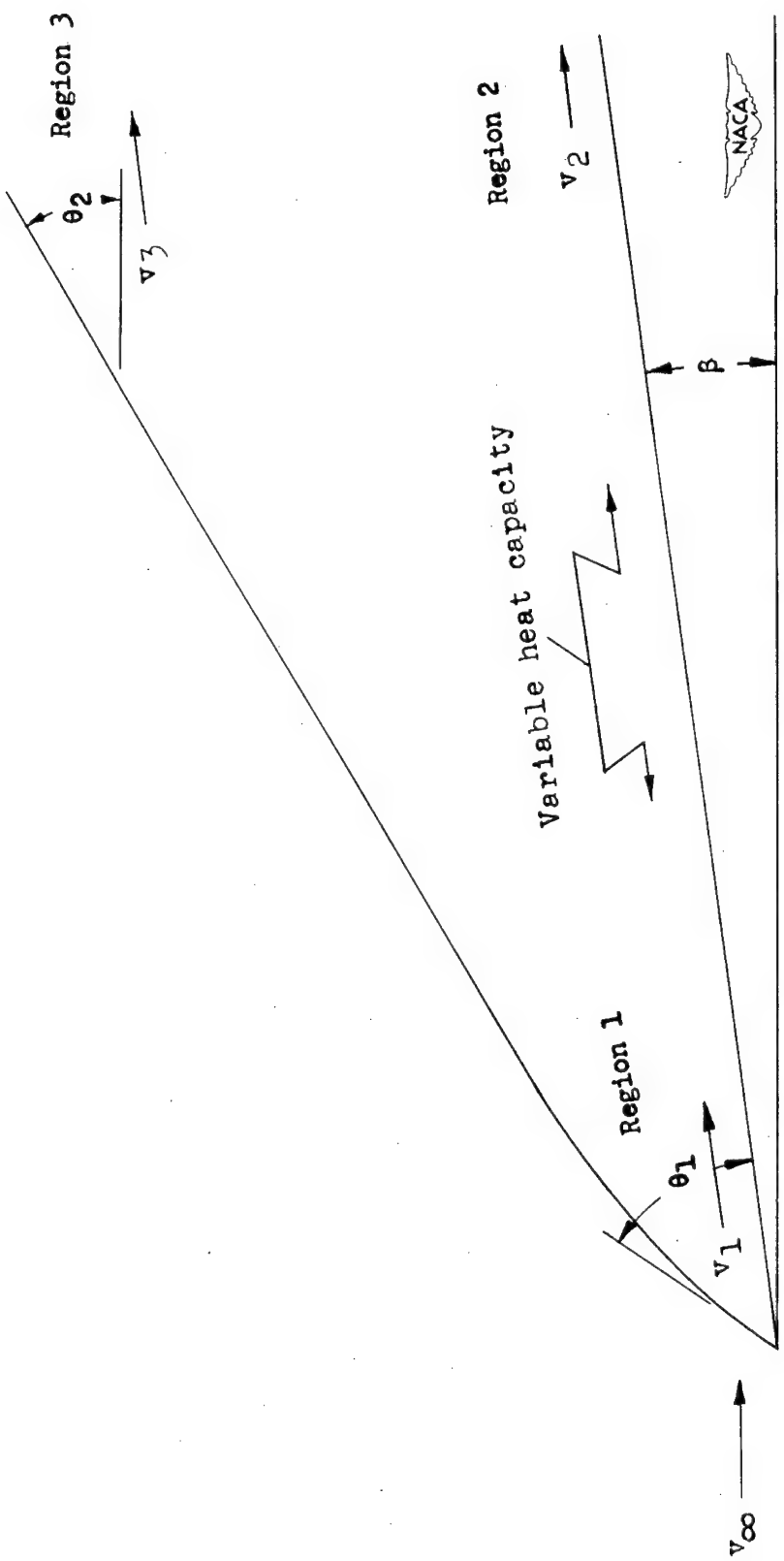

Figure 1.- Location of regions to be investigated.

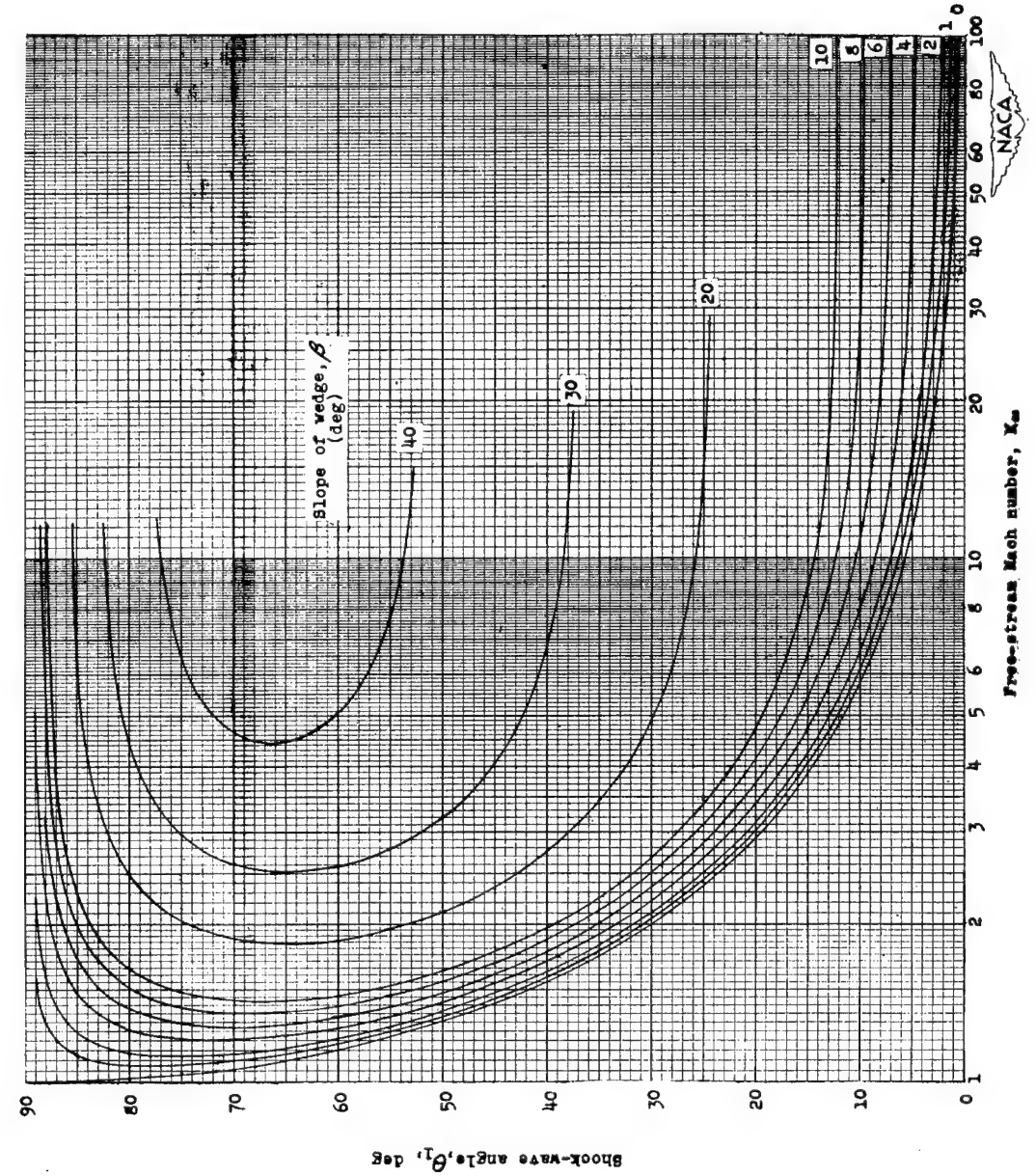

Figure 2.- Shock-wave angle for $\gamma = 1.4$.

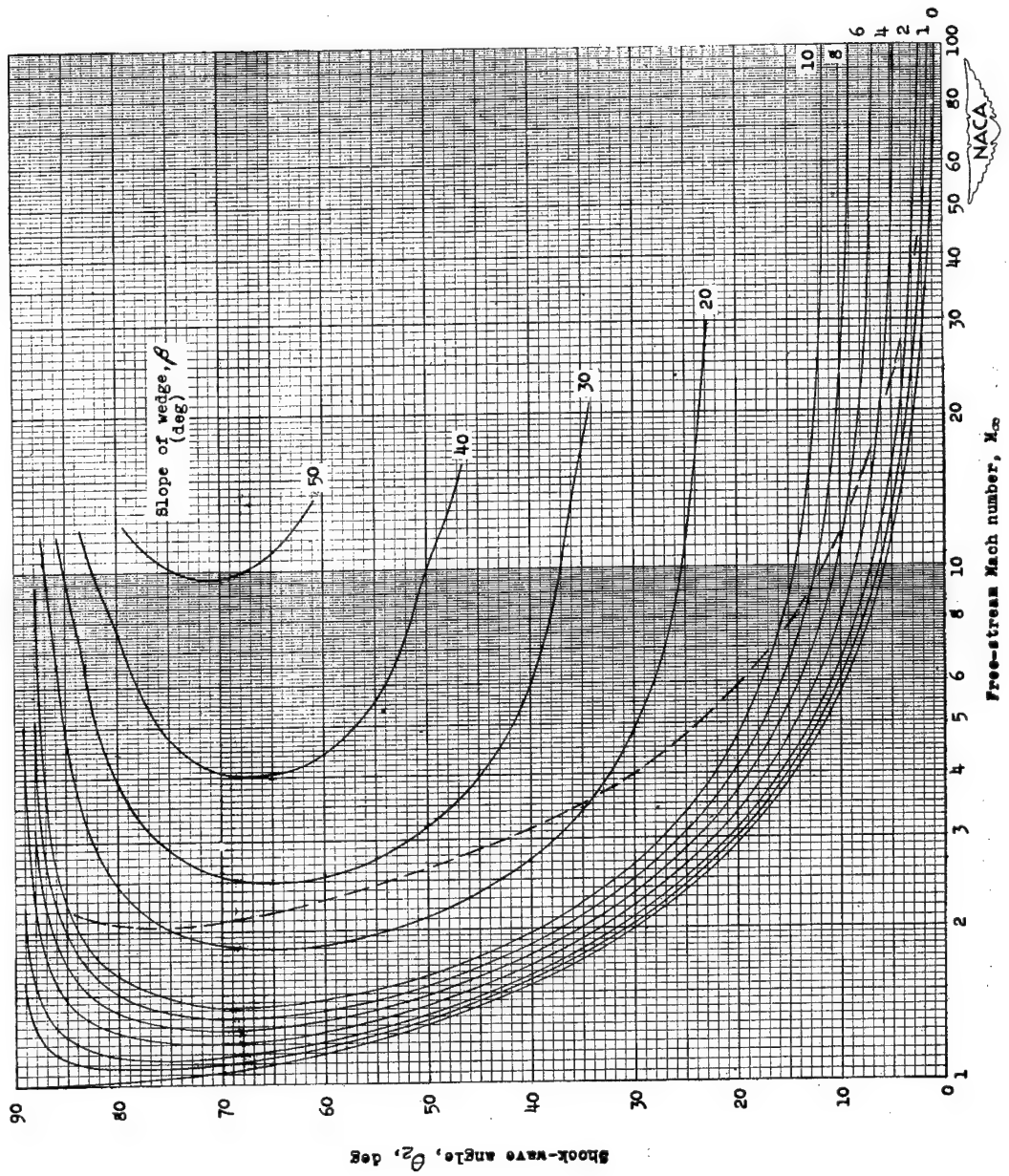

Figure 3.- Shock-wave angle for equilibrium specific heats.

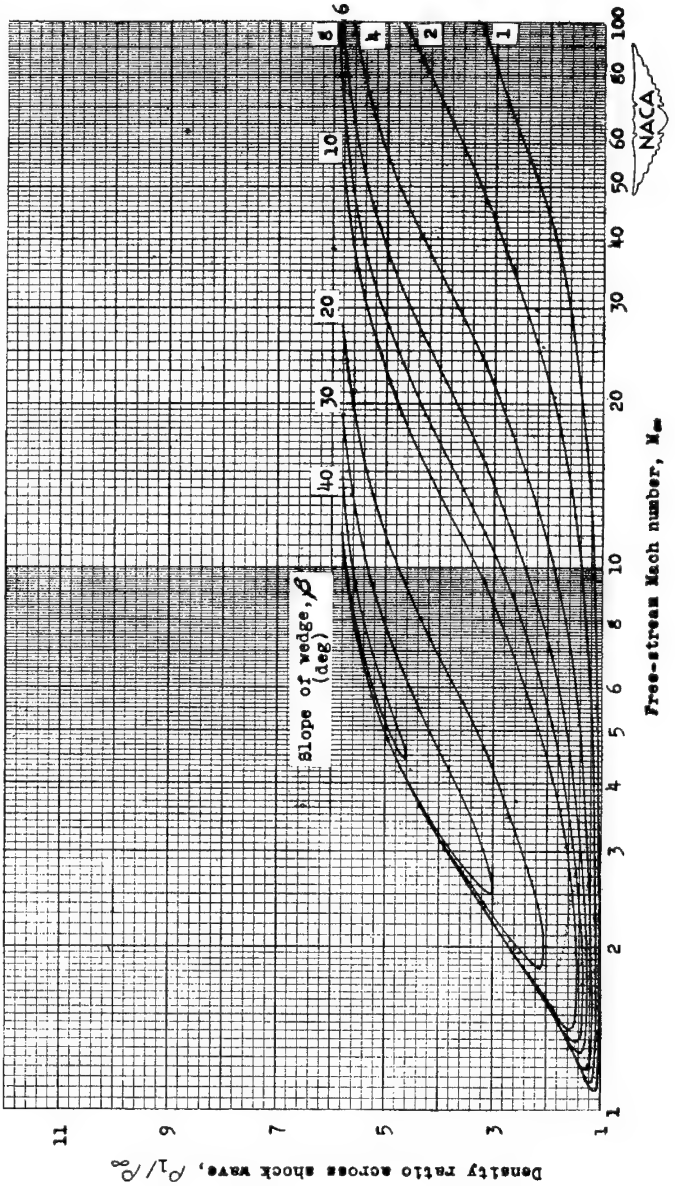

Figure 4.- Density ratio for $\gamma = 1.4$.

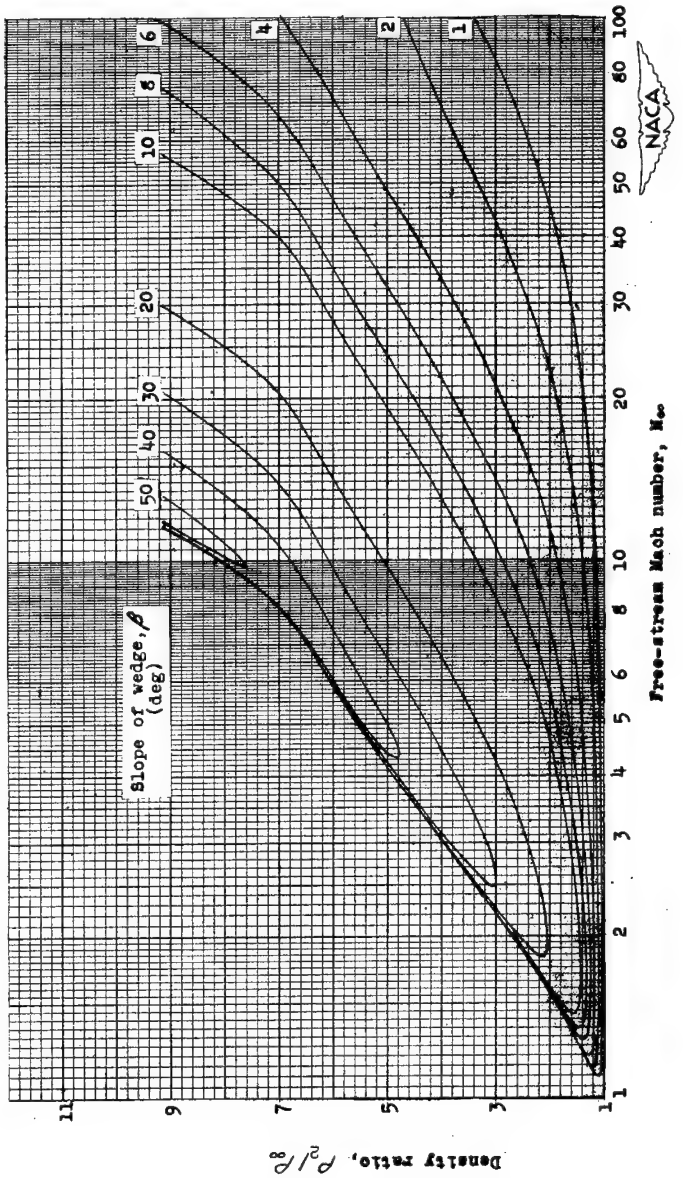

Figure 5.- Density ratio for equilibrium specific heats.

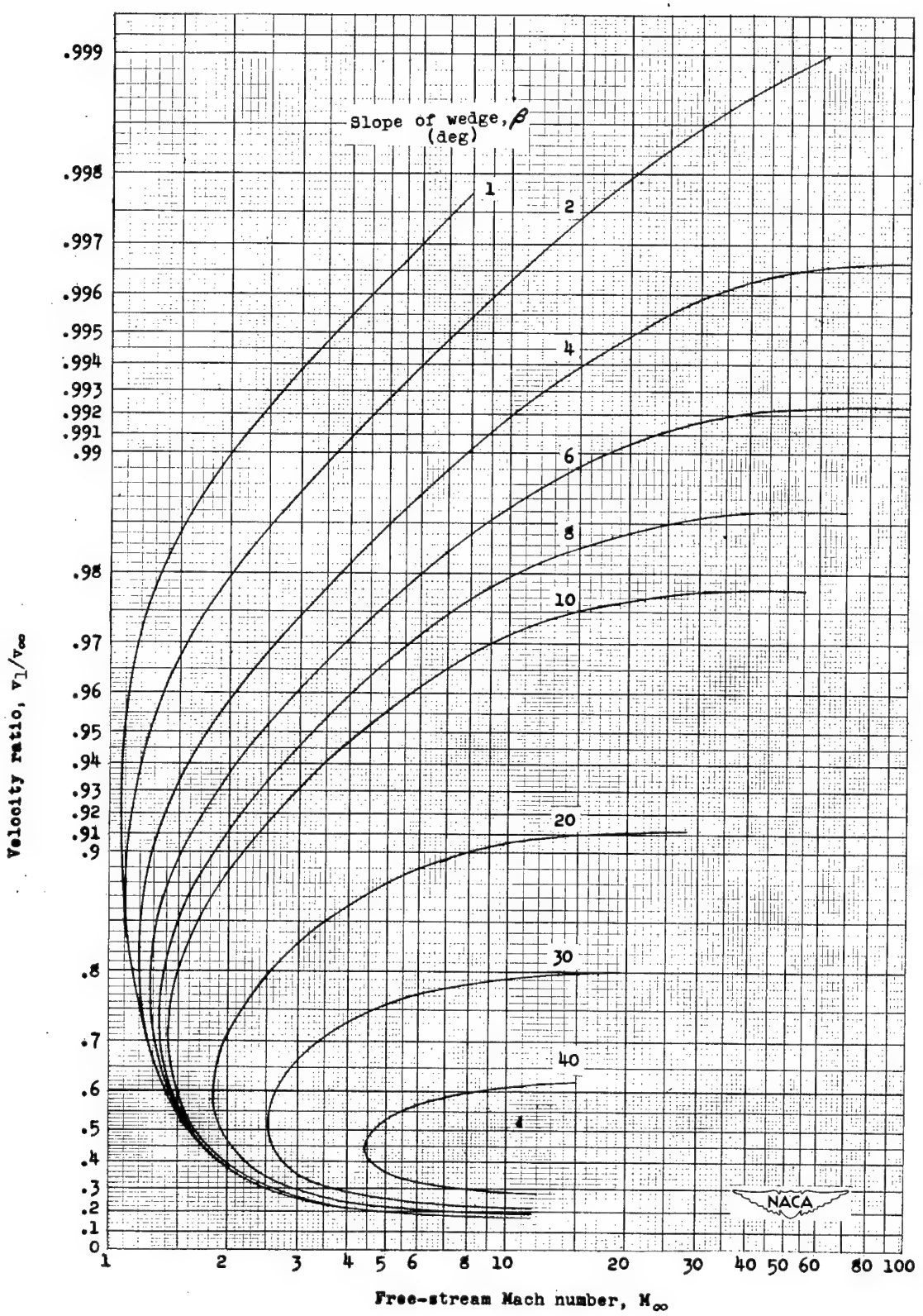

Figure 6.- Velocity ratio for $\gamma = 1.4$.

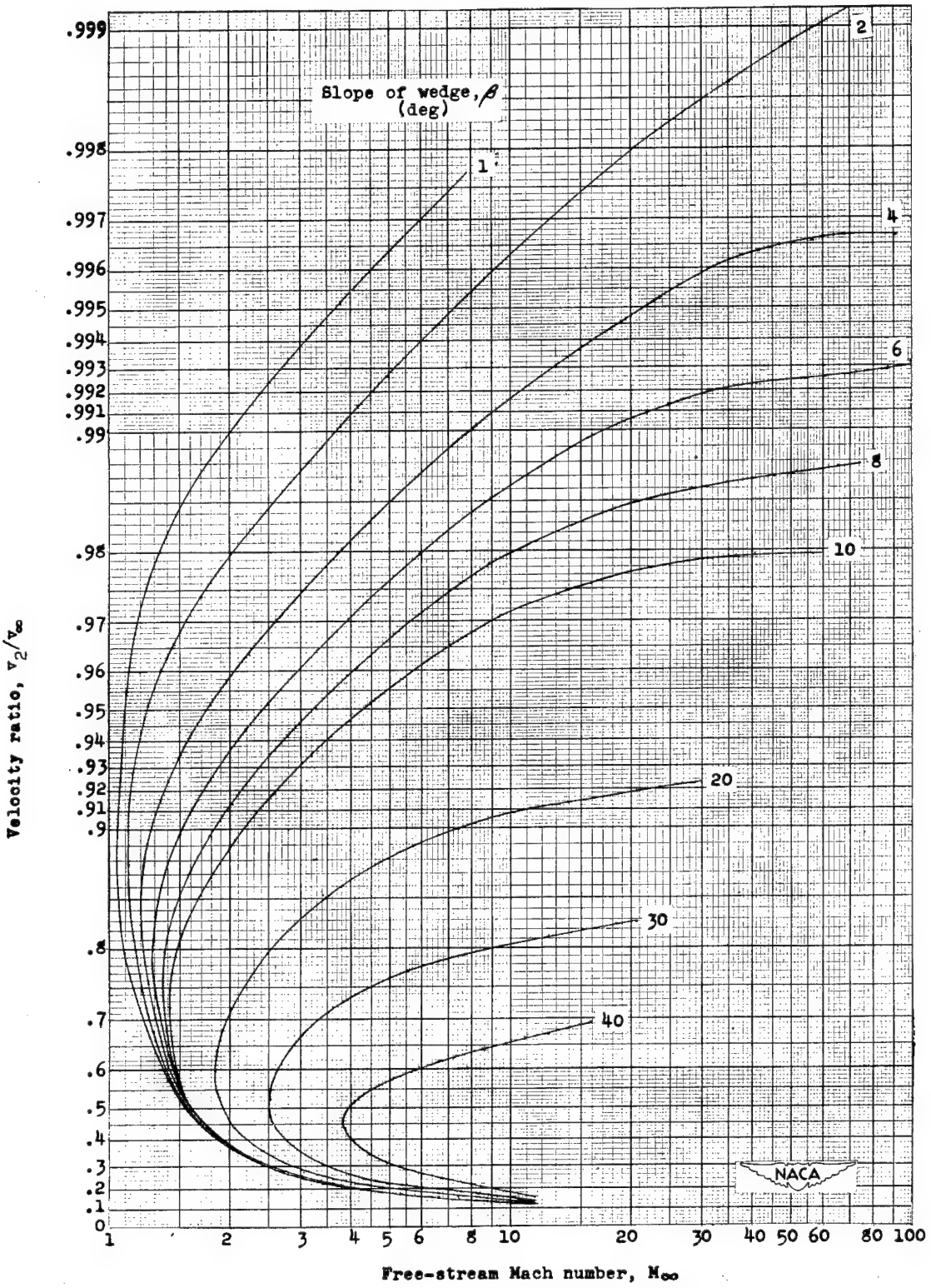

Figure 7.- Velocity ratio for equilibrium specific heats.

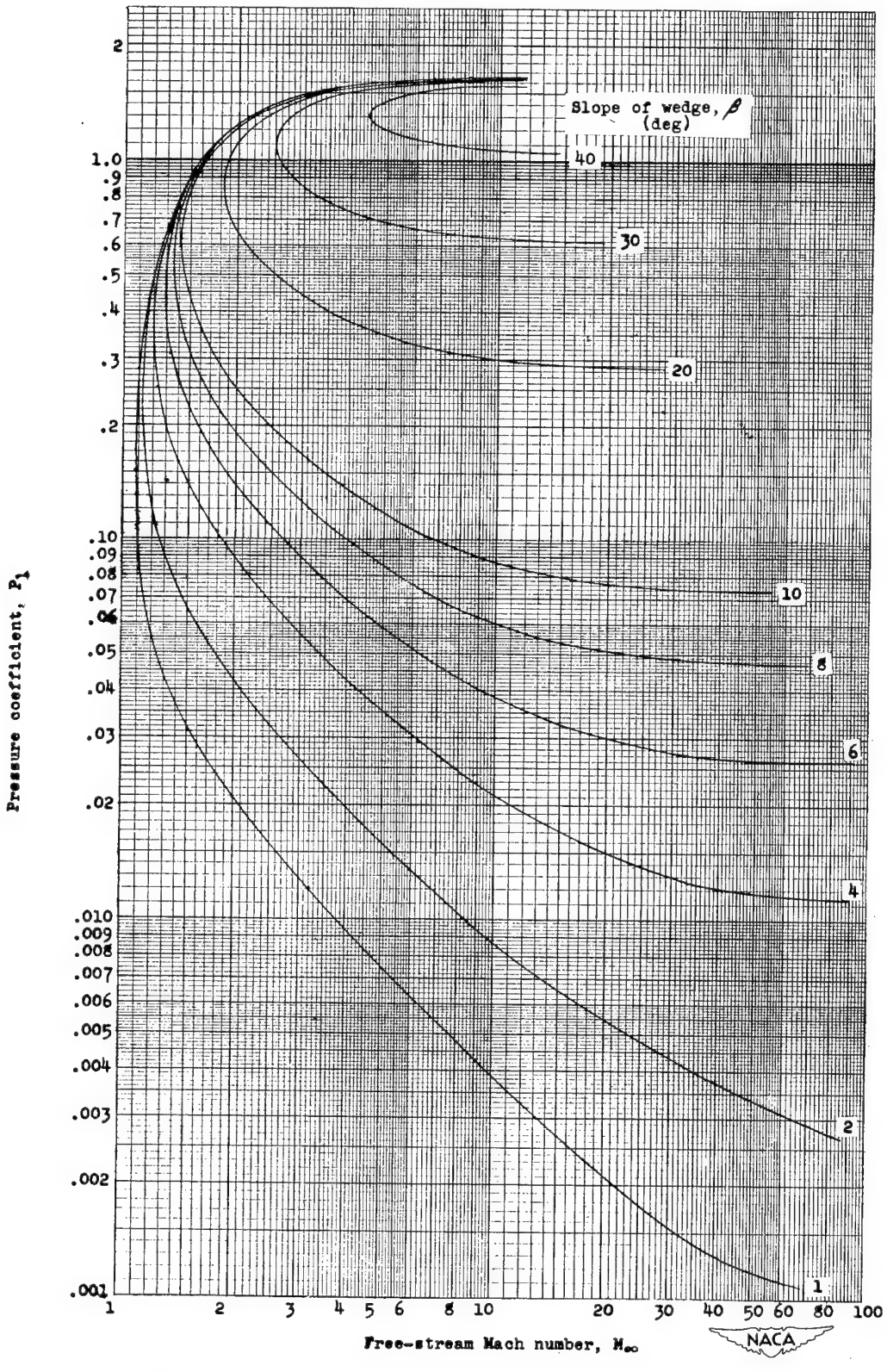

Figure 8.- Pressure coefficients for $\gamma = 1.4$.

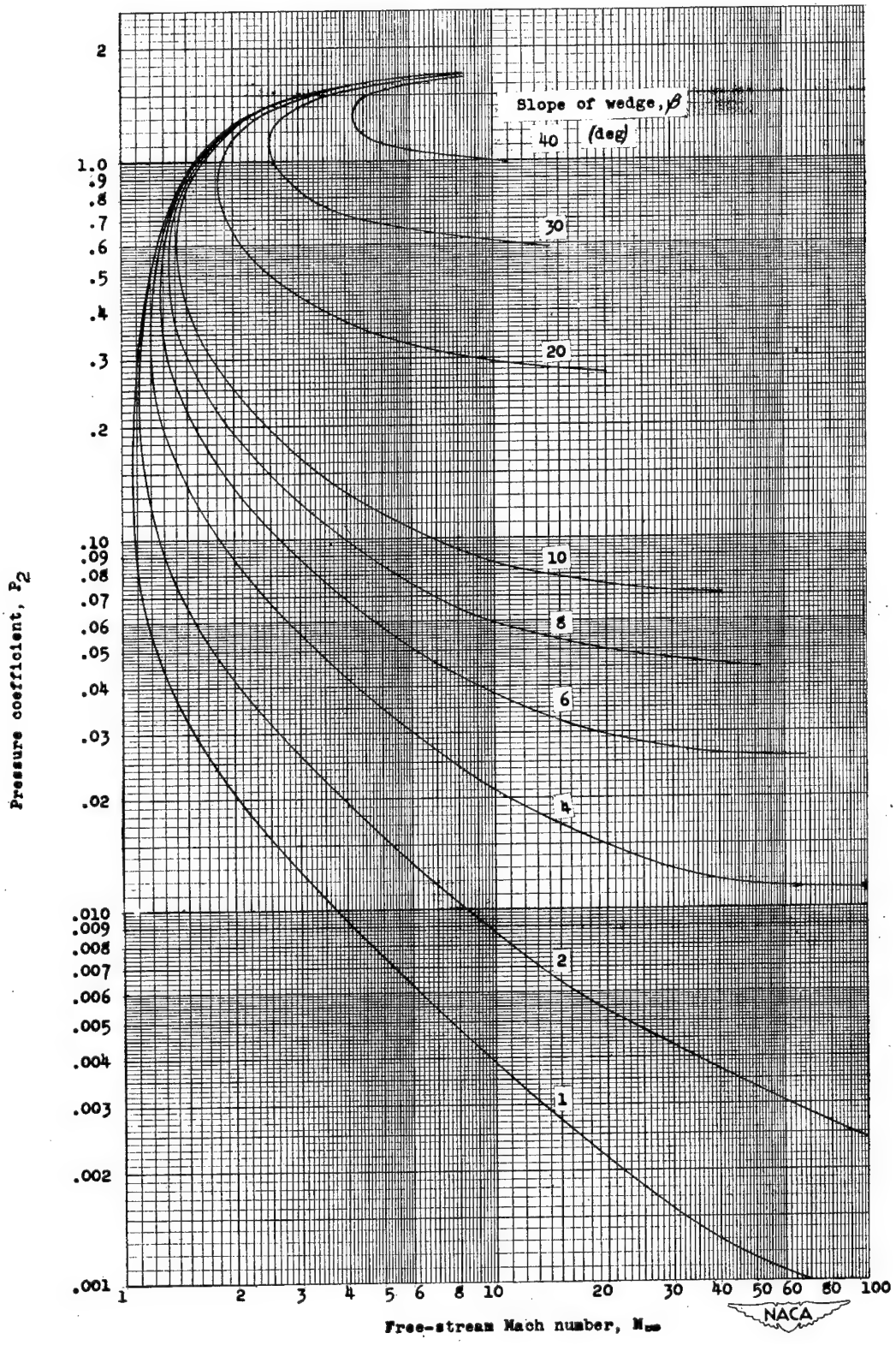

Figure 9.- Pressure coefficients for equilibrium specific heats.

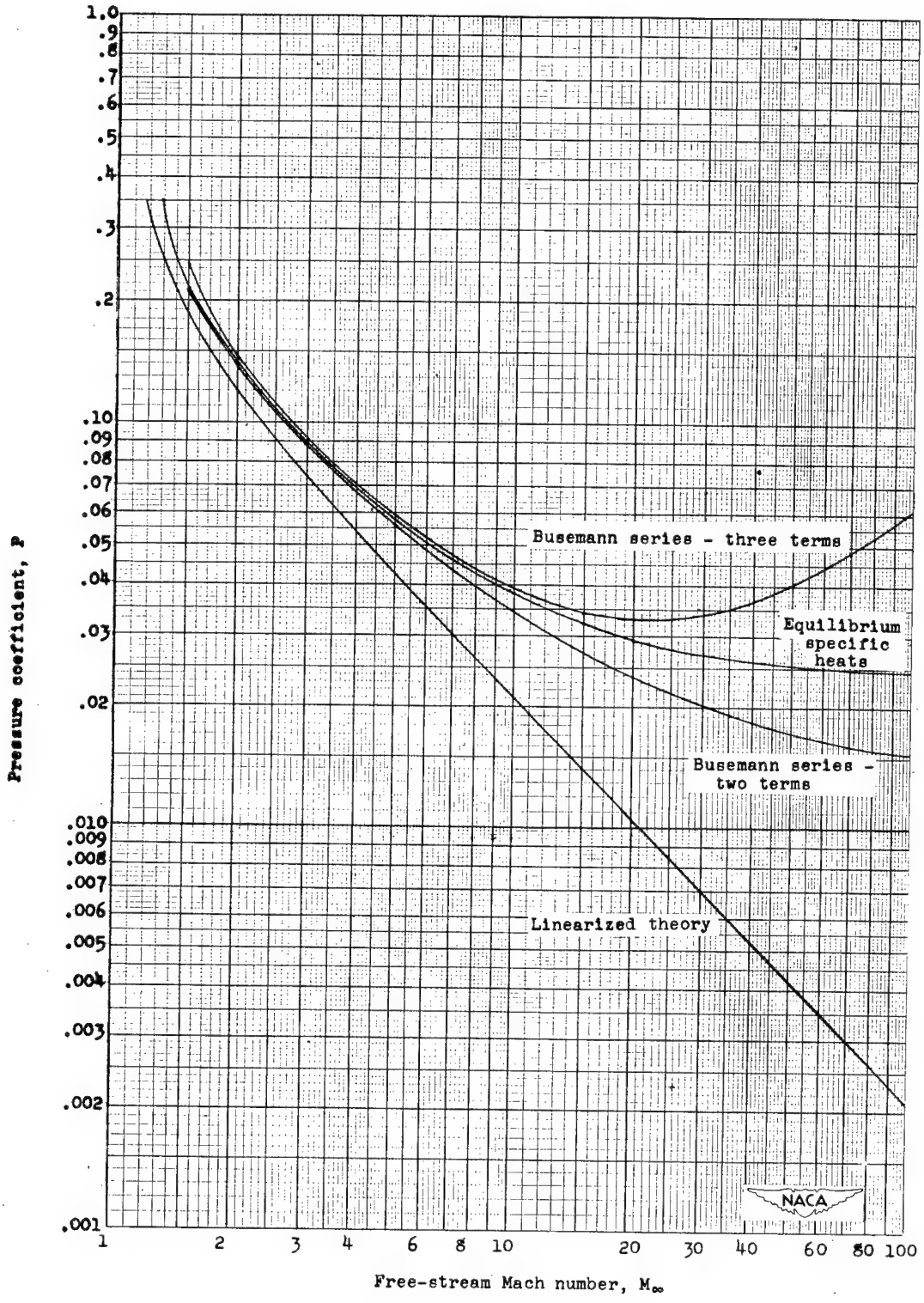

Figure 10.- Comparison of pressure coefficients calculated by existing approximate methods and by equilibrium specific-heats shock-wave equations. $\beta = 6^\circ$.

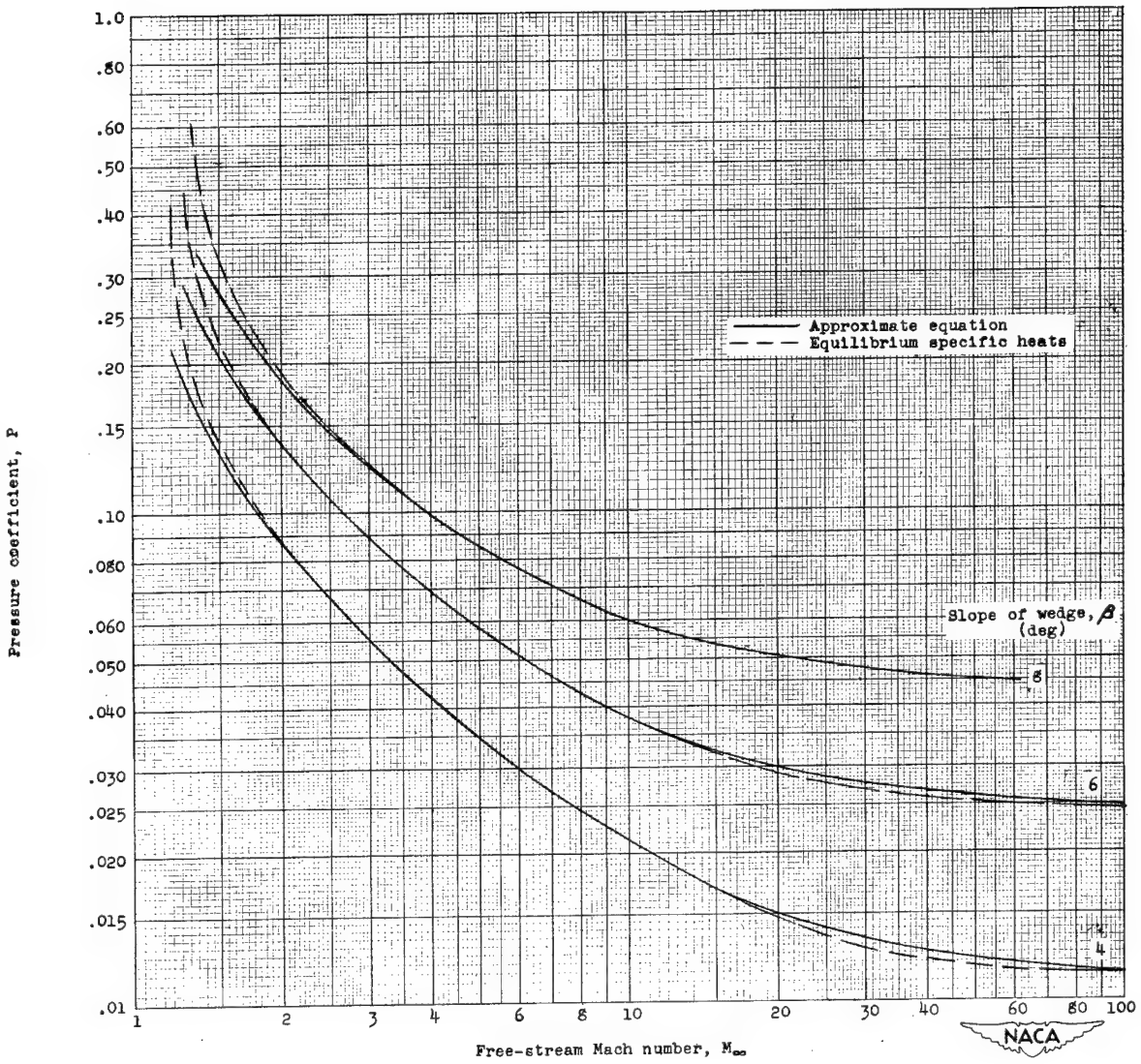

Figure 11.- Comparison of pressure coefficients calculated by approximate equation and by equilibrium specific-heats shock-wave equations.

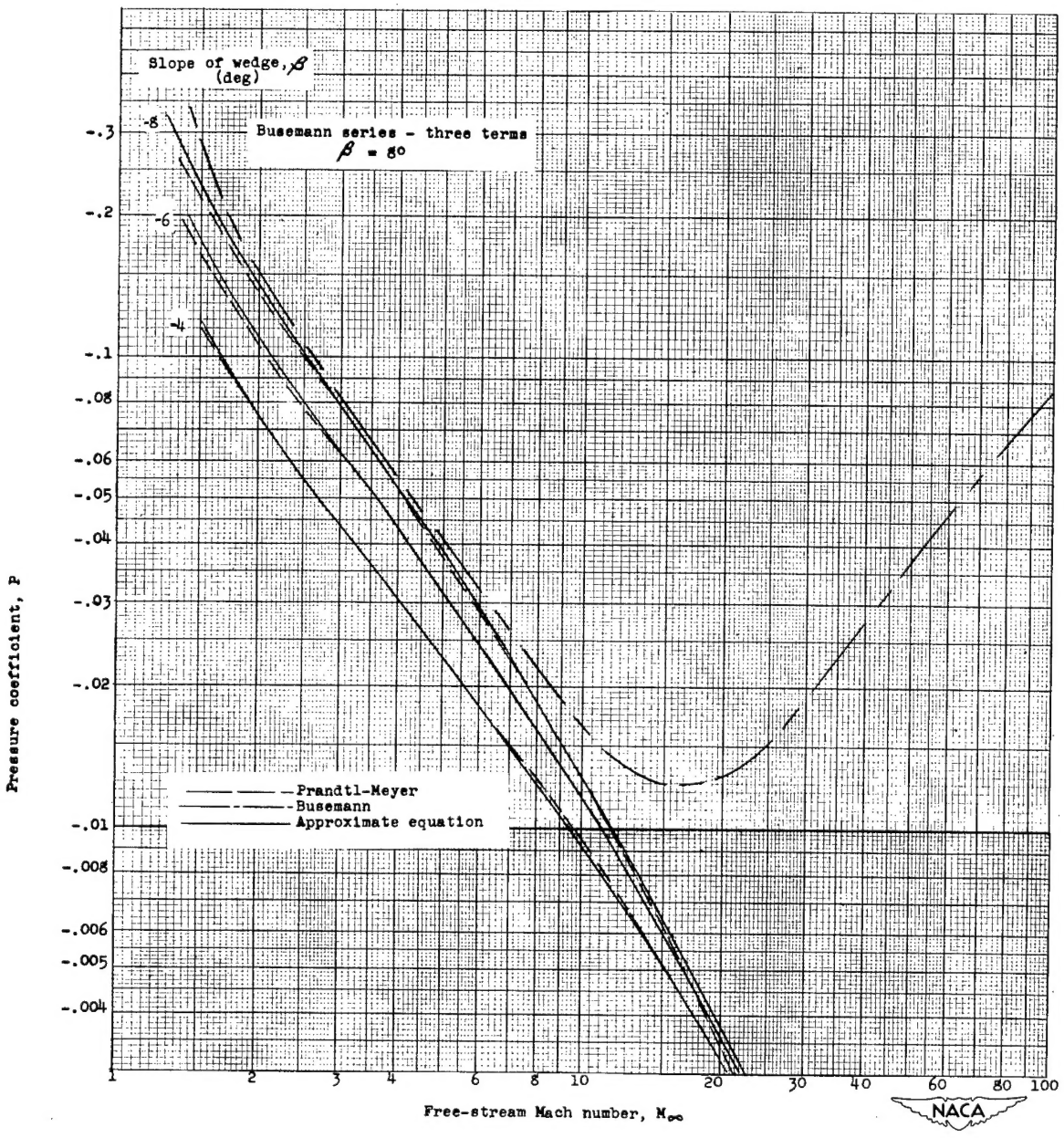

Figure 12.- Comparison of the expansion pressure coefficients calculated by the exact Prandtl-Meyer equations, by the Busemann third-order equation, and by the present approximate equation.

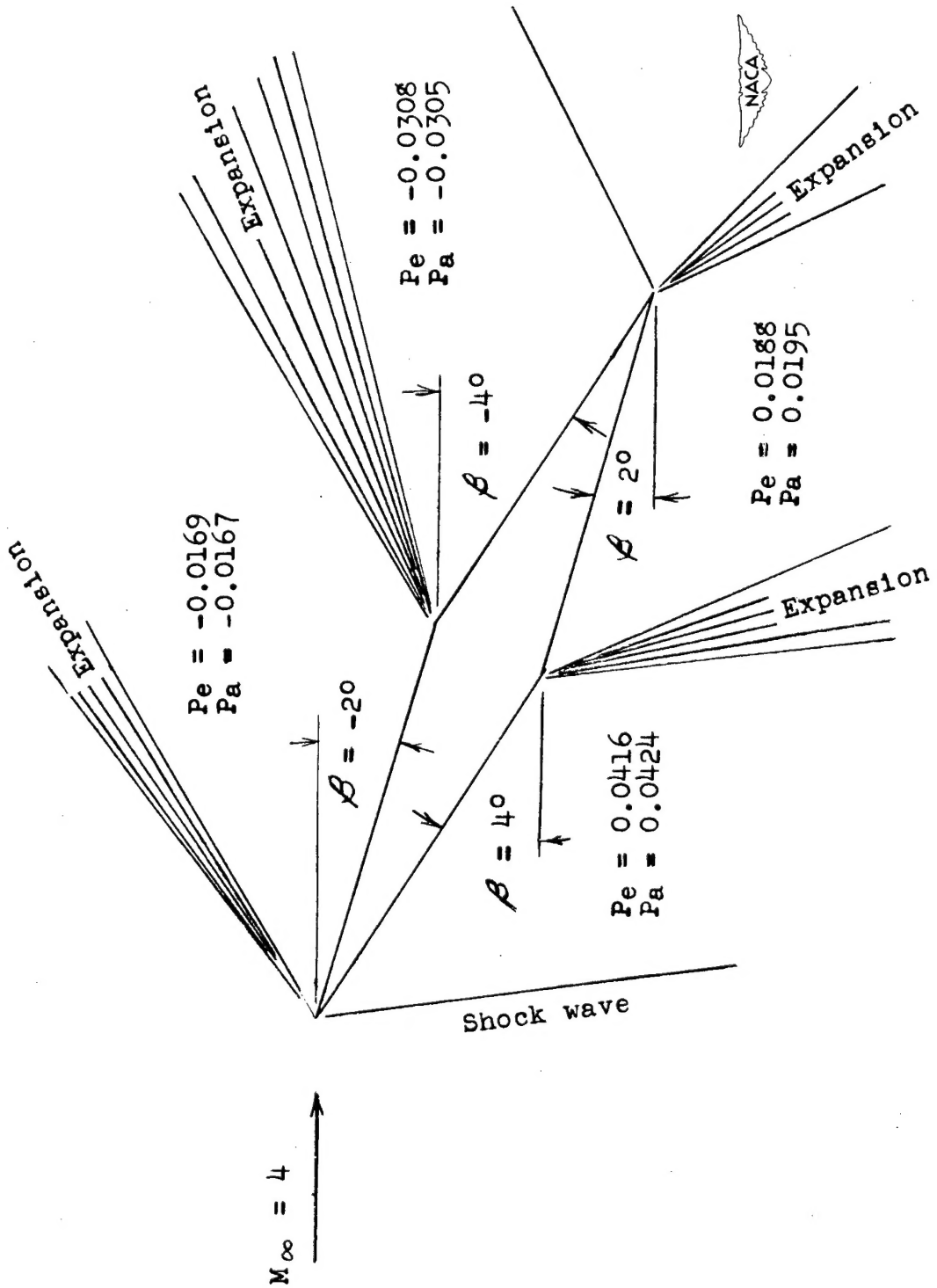

Figure 13.- Comparison of pressure distribution calculated by the exact and approximate methods for a 2° wedge airfoil at $M_\infty = 4$.

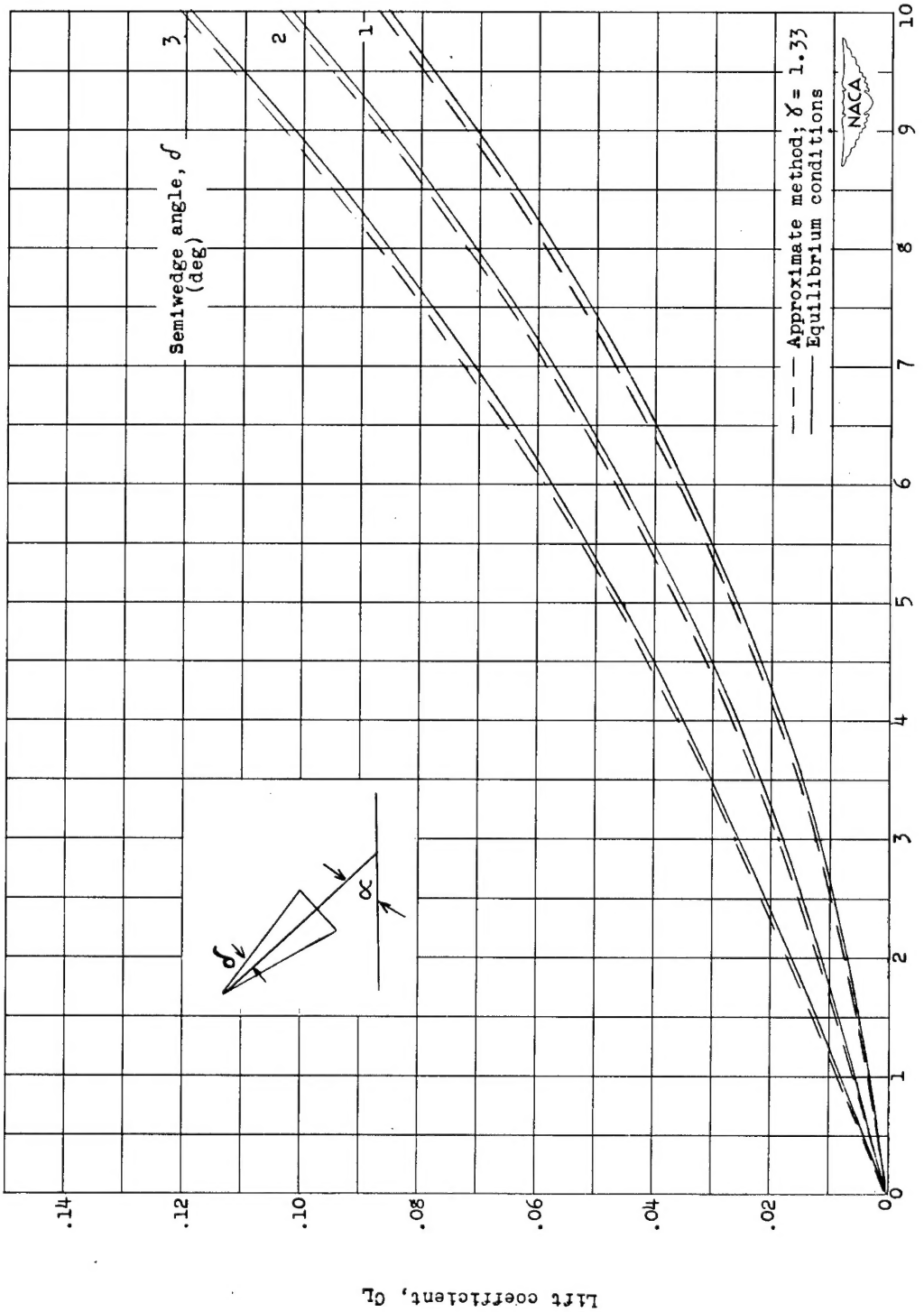

Figure 14.- Lift coefficient for a wedge airfoil. $M_\infty = 50$.

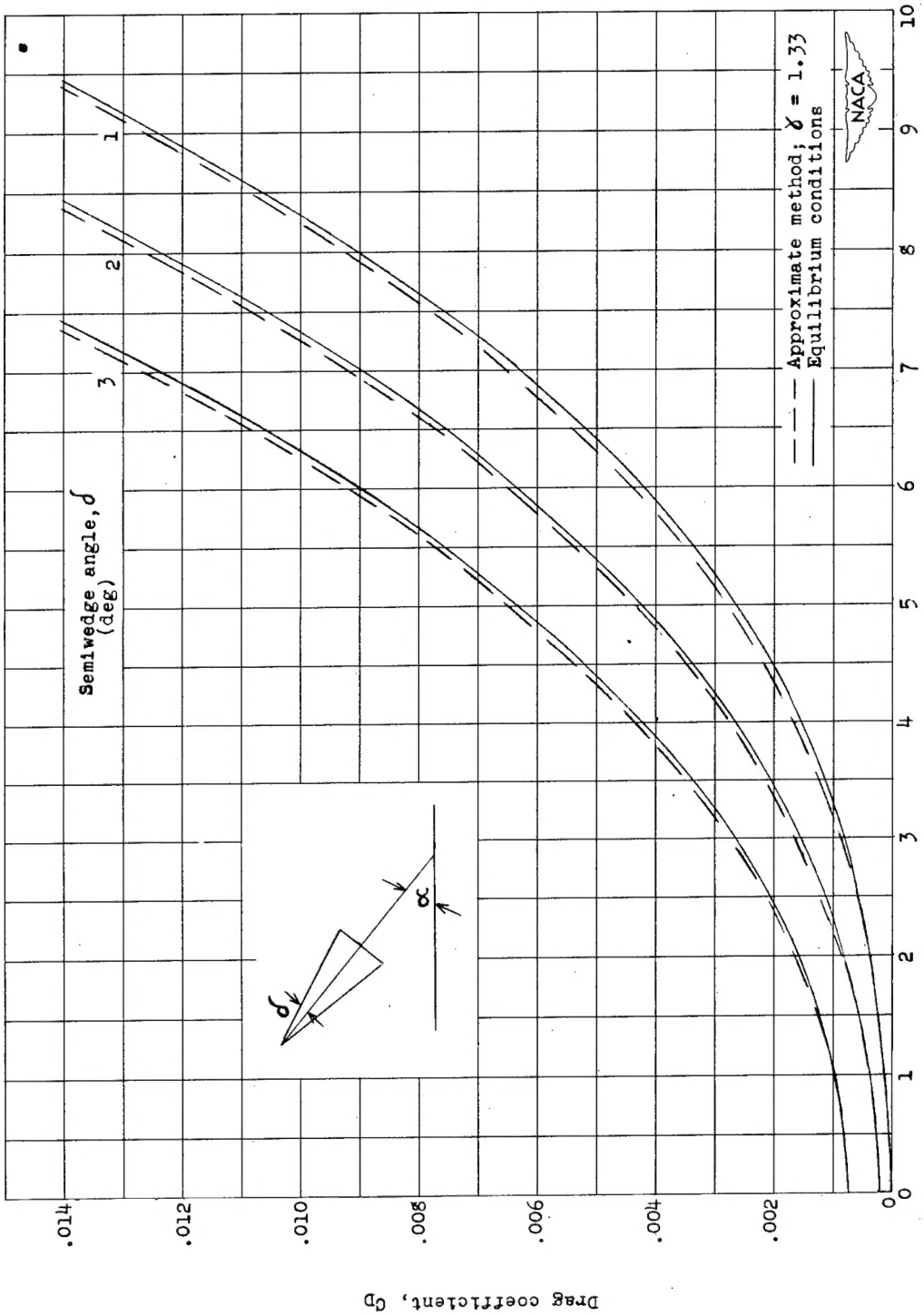

Figure 15.- Drag coefficient for a wedge airfoil. $M_\infty = 50$.